Volume 305, number 2, 105–109 FEBS 11201 June 1992

^{1}H NMR study on the conformation of bacitracin A in aqueous solution

Naohiro Kobayashi[a], Takato Takenouchi[a], Satoshi Endo[b] and Eisuke Munekata[a]

[a]*Institute of Applied Biochemistry, University of Tsukuba* and [b]*Tsukuba Research Laboratories, Takeda Chemical Industries Ltd., Tsukuba 305, Japan*

Received 6 January 1992; revised version received 5 May 1992

The conformation of bacitracin A, a widely used cyclic dodecapeptide antibiotic in aqueous solution, has been investigated using 500 MHz ^{1}H NMR and molecular modeling. Findings revealed that a region (residues 1-6) is folded over the cyclic ring, resulting in metal coordination sites, a thiazoline ring, and Glu[4] and His[10] being proximate to each other.

Bacitracin A; ^{1}H NMR; Energy minimization; Molecular dynamics; Three dimensional structure

1. INTRODUCTION

Bacitracin A (Fig. 1), a cyclic dodecapeptide produced by *Bacillus licheniformis*, possesses potent antibiotic activity against Gram-positive bacteria. This peptide has unusual amino acids, D-Glu, D-Orn, D-Phe and D-Asp, and a thiazoline moiety, and the side chain of L-Lys[6] is linked to the carboxyl terminus. Storm and Strominger [1] have shown that bacitracin A tightly binds C_{55}-isoprenyl pyrophosphate, a precursor unit of membrane-lipid biosynthesis, in the presence of bivalent metal cations such as Zn^{2+} and Mg^{2+} under neutral pH conditions. Recently, Scogin et al. [2] demonstrated that three groups in bacitracin A are involved in metal coordination; the carboxyl group of glutamic acid, the thiazoline ring and the histidine imidazole. To understand the detailed mechanisms underlying bacitracin A's biological actions and the complex formation between bacitracin A and bivalent metal cations or isoprenyl pyrophosphate, a precise conformation analysis of bacitracin A is required.

In this study, the conformation of bacitracin A in aqueous solution was investigated by proton 2D NMR techniques and molecular modeling.

2. MATERIALS AND METHODS

2.1. *Preparation of bacitracin A solution*

Bacitracin A was purchased from Wako Chemicals Co. and purified by reverse-phase HPLC. The peptide was dissolved in H_2O and the pH of the solution was adjusted to 7.0 and treated with Chelex 100 resin to remove polyvalent cations.

Abbreviations: NOE, nuclear Overhauser enhancement; NOESY, two-dimensional nuclear Overhauser enhancement spectroscopy; ROESY, rotating frame NOESY; RMSD, root mean square distance.

Correspondence address: E. Munekata, Institute of Applied Biochemistry, University of Tsukuba, Tsukuba 305, Japan.

2.2. *NMR measurements and molecular modeling*

For NMR measurements, 0.03–20 mM solutions of peptide in 90% ^1H_2O/10% ^2H_2O, (pH 2.8, 3.2 and 3.5) and ^2H_2O, (pH 3.0, 3.2 and 3.7) were used. The given pH refers to a direct reading without correction for the isotope effect.

All ^{1}H NMR spectra (500.137 MHz) were measured on a Bruker AM 500 spectrometer linked to an Aspect 3000 computer and a digital phase shifter at 298 and 303 K. Sodium-3-trimethyl-silyl propionate-d, (TSP) was used as a reference for all spectra.

All phase-sensitive 2D NMR spectra were recorded in the pure-phase absorption mode using the time-proportional phase incrementation method [3]. They include DQF-COSY [4], HOHAHA spectra [5] with mixing times of 47 ms and 81 ms, NOESY spectra [6] and ROESY spectra [7]. NOESY and ROESY spectra were recorded at mixing times of 100–600 ms, and 100–250 ms respectively, to confirm the linearity of the NOE and ROE buildup.

Solvent suppression was achieved by irradiating the H_2O peak during the relaxation delay (1.5–2.0 s) in ^1H_2O and in NOESY experiments during the mixing time as well.

Data was accumulated from 32 scans and 4 dummy scans into 4 K data points in the DQF-COSY and HOHAHA experiments, and into 2 K data points in the other 2D experiments. In most cases, 256–512 free induction decays (FIDs) were recorded and zero-filled into 1 K data points in the t1 direction. Spectral widths of F1 and F2 directions were set at 10 ppm for ^2H_2O and at 14 ppm for ^1H_2O. Prior to Fourier transformation, the FIDs were multiplied by a squared cosine-bell weighting function in the t1 and t2 directions.

Energy minimization [8] and molecular dynamics calculation [9], and graphics were performed on a TITAN 750 workstation using the NMRGRAF program with Dreiding force field [10].

3. RESULTS

For all 2D spectra, 10 mM sample of bacitracin A was used. 1D spectrum of the 0.03 mM sample showed substantially the same spectral pattern as that of the 10 mM sample, confirming the absence of any significant aggregation in this concentration range.

The assignments of the proton resonances of the peptides were carried out through the analysis of DQF-COSY, HOHAHA, NOESY and ROESY spectra. Since Leu[3], Glu[4], Lys[6], and Orn[7] residues and the thia-

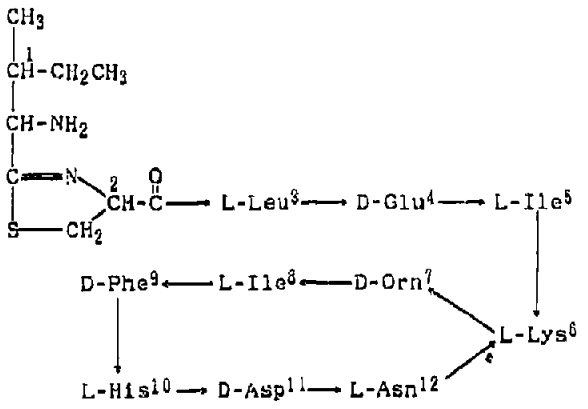

Fig. 1. Structure of bacitracin A.

zoline moiety possess characteristic spin systems, the proton resonances of these residues were easily assigned. Sequential assignments [11] were achieved by the NOESY and ROESY spectra in ^1H_2O and ^2H_2O. Fig. 2 shows the NOESY spectrum of bacitracin A measured at a mixing time of 400 ms in $^1H_2O/^2H_2O$ (9:1), pH 3.2 and 303 K. Chemical shifts of assigned proton resonances are listed in Table I and a summary of the observed NOE connectivities are shown in Fig. 3.

H–D exchange rates of amide protons are closely related to hydrogen bonding or shielding from the solvent. The peptide previously lyophilized from ^1H_2O solution was dissolved in ^2H_2O at pH 3.0 and the amide proton signals were measured immediately. Most of the amide proton signals disappeared within 2 min, while the half-lives of Lys^6 ε NH were 16 min.

In the NOESY and ROESY experiments, NOE and ROE intensities increased linearly up to a mixing time of 400 and 150 ms, respectively. Thus, the NOE and ROE obtained at these mixing times were converted into proton–proton distance in angstroms, accurate to one decimal place [12]. The known distance between the geminal protons of Cys^2 CβH$_2$ was taken to be 1.8 Å.

The proton–proton distances obtained were classified into three groups, 2.2 Å$\leqq$ d $\leqq$ 3.5 Å, 3.6 Å$\leqq$ d$\leqq$ 3.9 Å and 4.0 Å$\leqq$ d$\leqq$ 4.5 Å, and the upper and lower limits for the groups were set to −0.3 Å and +0.3 Å, −0.4 Å and +0.4 Å, −0.6 Å and +0.8 Å, respectively [13]. The lower limits assigned shorter than 2.0 Å were commonly set to 2.0 Å. In total 32 intra-residual, 22 sequential and 8 long-range NOE-redived distance constraints were used for energy minimization and molecular dynamics calculations.

By running a 20 ps molecular dynamics calculation which neglected the non-bonding energy terms in the Dreiding force field, 20 structures were extracted from the trajectory at 1 ps intervals, and were subjected to energy minimization with regard to non-bonding energy terms. Then 17 structures were selected for simulating annealing as the initial structure, except for three structures which revealed significantly high van der Waals energy.

For the constrained energy minimization and molecular dynamics, electrostatic and hydrogen bonding terms were eliminated from the Dreiding force field. The dihedral angles of peptide bond (all *trans*) and the chirality of asymmetric heavy atoms were commonly restrained by the harmonic potential throughout all calculations. Square-well effective potentials were included in the calculations as the constraints for the inter-proton distances determined by the NOESY and ROESY experiments.

$$E_{NOE} = \begin{cases} K(x_i - x_i^u)^2 & \text{if } x_i > x_i^u \\ 0 & \text{if } x_i^l \leqq x_i \leqq x_i^u \\ K(x_i - x_i^l)^2 & \text{if } x_i < x_i^l \end{cases}$$

where x_i is the calculated value of inter-proton distances and x_i^l and x_i^u are the upper and lower limits of the target

Table I

Chemical shifts (ppm) of proton resonances of bacitracin A in 90% ^1H_2O/10% ^2H_2O at pH 3.2, 303 K

Residue	NH	CαH	CβH	Other
L-Ile^1	a	4.35	2.09	CγH 1.31, 1.50; CγH$_3$ 1.07; CδH$_3$ 0.97
L-Cys^2	–	5.28	3.59, 3.79	
L-Leu^3	8.16	4.52	1.61, 1.61	CγH 1.71; CδH$_3$ 0.89, 0.94
D-Glu^4	8.67	4.43	2.01, 2.16	CγH$_2$ 2.46, 2.46
L-Ile^5	8.07	4.16	1.65	CγH$_2$ 1.14, 1.39; CγH$_3$ 0.85; CδH$_3$ 0.83
L-Lys^6	8.29	4.31	1.82, 1.82	CγH$_2$ 1.33, 1.34; CδH$_2$ 1.52, 1.52 CεH$_2$ 3.20, 3.28; NεH 7.83
D-Orn^7	8.11	4.48	1.70, 1.70	CγH$_2$ 1.77, 1.86; CδH$_2$ 3.04, 3.04; NδH 7.58
L-Ile^8	8.17	4.17	1.72	CγH$_2$ 0.99, 1.22; CγH$_3$ 0.60; CδH$_3$ 0.76
D-Phe^9	8.55	4.65	2.90, 3.19	C2, 6H 7.22; C3, 5H 7.31; C4H 7.26
L-His^{10}	8.59	4.82	3.03, 3.30	C2H 8.55; C4H 7.03
D-Asp^{11}	8.75	4.73	2.79, 2.87	
L-Asn^{12}	8.61	4.70	2.83, 2.91	NδH 7.12, 7.59

Stereospecific assignments of the diastereomeric proton signals have not been determined. The signal labeled 'a' was not detectable under these experimental conditions.

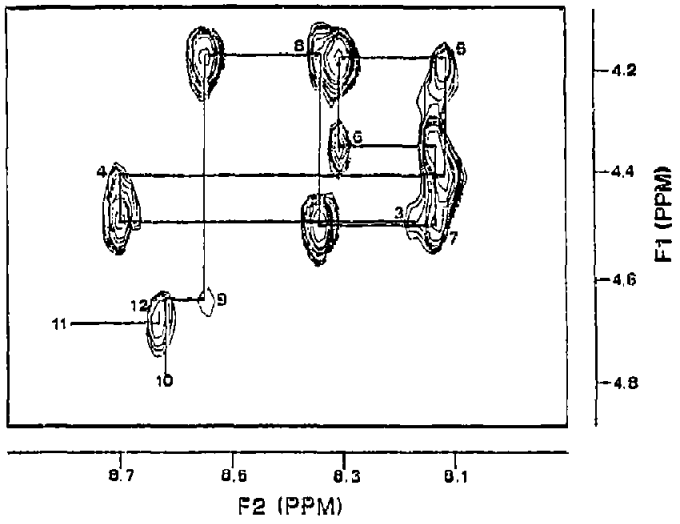

Fig. 2. CαH–NH region of the NOESY spectrum of bacitracin A measured at a mixing time of 400 ms. The sequential connectivities are indicated by the solid lines labeled with the residue number of NH resonance.

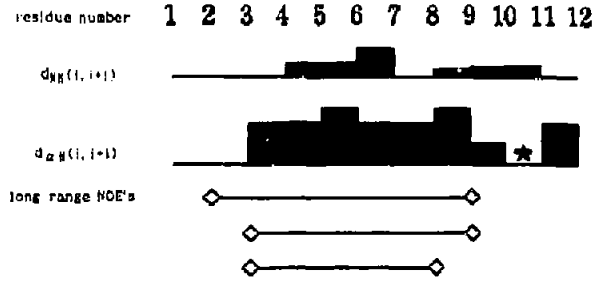

Fig. 3. Summary of the observed NOE connectivities obtained from the 500 MHz NOESY spectrum shown in Fig. 2. The intensity of the observed NOEs are represented by the height of the bar. ★ indicates that NOE cross peaks could not be observed due to a strong water signal.

ranges of inter-proton distances derived from observed NOE or ROE. The force constant is expressed as K. When x_i is longer than 8.0 Å or shorter than 2.0 Å, the E_{NOE} is switched to a linear potential. For the NOE distance constraint, including the pseudostructures in which the stereospecific assignments were not obtained, the correction factors established by Wüthrich et al. were applied [11]. The pseudostructures of the methyl protons were regarded as united atoms and distance contraints were set on the carbon atom using the above correction factor without any modification. Constrained molecular dynamics calculations were performed at 1,000 K with a time step of 1 fs by using annealed NOE restrains, programmed protocol in NMRGRAF. In each annealing routine, the force constant K was increased by 20 kcal·mol^{-1}·Å^{-2} every 0.1 ps and continued until a maximum force constant of 100 kcal·mol^{-1}·Å^{-2} was reached. Thus the process was reversed by continually decreasing the force constant, K, from 100 to 0 kcal·mol^{-1}·Å^{-2}. The period of each annaeling routine was 1 ps and conformational data were similar stored to the trajectory at the end of the routine. This protocol is somewhat similar to standard simulating annealing methods using increment or decrement of simulating temperatures [14]. Recently, some reports demonstrated molecular dynamics simulation with stepwise changing of the NMR force constant in order to overcome local minimum of conformational energy [15,16].

25 conformers with lower rms violation (root mean square difference between inter-proton distances of the calculated structures and experimental constraints) were extracted from 170 conformers of 17 trajectories. Finally, constrained energy minimizations followed, and six final structures derived from different initial structures were obtained. The criteria for selecting the six final structures were lower van der Waals energy, <150 kcal·mol^{-1}, maximum violation of upper distance limits, <0.5 Å, and lower rms violation, <0.2 Å. The maximum violation of upper distance limits and rms violation of the six structures are listed in Table II. Root mean square distance (RMSD) values between all pairs of the six structures, deleted of all protons, and average RMSD values of six final structures (1.62 Å) are also

Table II

Average RMSD, rms violations and maximum violation of the final six structures

Å	average (range)
Average RMSD	1.62
Number of residual distant constraint violation > 0.2 Å	5.1 (4–6)
Rms violation	0.09 (0.08–0.10)
Maximum violation	0.48 (0.52–0.46)

The average root mean square distance (RMSD) is calculated for all pairs of the final six structures at the heavy atoms. Violation is the value of the difference between inter-proton distance of the final structure and the upper or lower limit of experimental constraints.

Table III

Calculated empirical energy and its variations of the final six structures

Energy term	Average (range) (kcal·mol^{-1})
Bond	38.93 (37.80–40.27)
Angle	232.70 (228.74–236.95)
Torsion	30.44 (27.92–33.98)
Inversion	2.17 (2.08–2.25)
van der Waals	133.91 (136.08–132.38)
Constraint	31.05 (21.45–40.25)

The value of the constraint comprises the square-well potential of NOE distance constraint, the harmonic potential of the torsion angle on the peptide bond and the harmonic potential of the inversion at the asymmetric carbon atoms calculated with force constants of 100 kcal·mol^{-1}·Å^{-2}, 20 kcal·mol^{-1}·Å^{-2}·rad^{-2}, and 40 kcal·mol^{-1}·Å^{-1}·rad^{-2}, respectively. The others are calculated with default values of the force constant in the Dreiding force field.

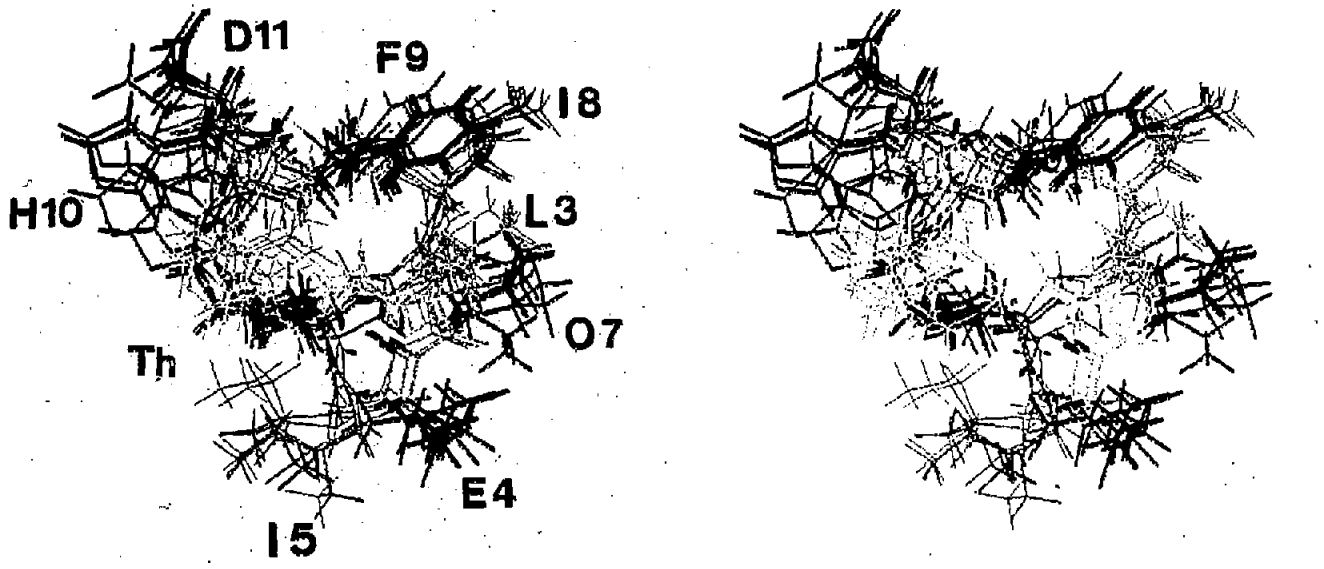

Fig. 4. Stereoview of the superimposed final six structures. The residues are indicated in capital letters and arbitrary numbers as in Fig. 1; D = Asp, E = Glu, F = Phe, H = His, I = Ile, L = Leu, N = Asn, O = Orn and Th = Thiazoline moiety.

shown in Table II. The conformational energy values, bond, angle, torsion, inversion, van der Waals and constraint, are shown in Table III. Fig. 4 shows the six final structures superimposed.

4. DISCUSSION

The precise structure of bacitracin A has not yet been reported. Recently, Pfeffer et al. [17] reported the X-ray structure of bacitracin A complexed to subtilisin proteinase, in which two bacitracin A molecules bind to two enzyme molecules. The conformation of the two bacitracins differs significantly in parts and has relatively high temperature factors indicating a certain amount of flexibility in their structures. The region of residues 1–6 is extended linearly in their structures. In our final structures, however, the region folds compactly. The reason for this discrepancy lies in the fact that the structures they studied were derived from a complex of bacitracin A with subtilisin, while our final structures were studied in aqueous solution.

In the final six structures, the region from Leu^3 to Phe^9 is seen as a common compact fold. Indeed, in NOESY and ROESY experiments, some long-range NOEs were observed between Leu^3, Ile^8 and Phe^9, therefore, these hydrophobic residues form a cluster.

The slow exchange of Lys^6 ε NH suggests that the NH proton forms a hydrogen bond. In the final six structures, the NH proton is directed to Asp$^{11}\alpha$ CO, apparently forming a weak hydrogen bond.

Regarding the dihedral angles (ϕ and ψ) among the final six structures (Table IV), Glu^4, Lys^6 and His^{10} are quite variable, because little NOE was observed in these residues. On the other hand, residues Leu^3, Ile^8 and Phe^9 are well converged due to many constraints, including long-range NOE.

It is known that the antibiotic activity of bacitracin A requires bivalent metal cations such as Zn^{2+} and Mg^{2+}, and considerable evidence has demonstrated that bacitracin A and metal cations form 1:1 complexes stoichiometrically. Scogin et al. [2] proposed a model for a bacitracin A–Zn^{2+} complex in which three metal coordination sites, the thiazoline ring, the carboxyl group of Glu^4, and His^{10} imidazole, are involved. In our study, all NOE data of bacitracin A were recorded at pH 3.2,

Table IV

Dihedral angles and their variations among the final six structures (degrees).

Residue	ϕ	ψ
L-Ile^1	–	151.7 ± 10.1
L-Cys^2	–	157.6 ± 12.0
L-Leu^3	−130.8 ± 8.1	40.6 ± 5.7
D-Glu^4	− 96.0 ± 18.8	−111.1 ± 12.0
L-Ile^5	− 76.0 ± 28.2	− 10.9 ± 32.1
L-Lys^6	−104.6 ± 40.3	− 15.5 ± 79.2
D-Orn^7	179.3 ± 41.1	−143.2 ± 19.3
L-Ile^8	−100.4 ± 23.5	132.2 ± 3.9
D-Phe^9	90.9 ± 4.6	− 86.5 ± 89.5
L-His^{10}	126.9 ± 71.2	− 21.2 ± 6.0
D-Asp^{11}	− 35.1 ± 1.8	− 66.8 ± 0.7
L-Asn^{12}	− 64.6 ± 7.5	–

For each angle, the range of values covered by the final six structures is represented by the center of the range and its size.

but bacitracin A does not bind bivalent metal cations under these conditions. It is of interest that the coordination sites proposed by Scogin et al. are proximate in the final six structures.

Hausmann et al. [18] reported that partial hydrolysis of bacitracin A gives the tetrapeptide, Phe- Ile-Cys-Leu, indicating the presence of a hydrogen bond between the N-terminal amino group of Ile^1 and the carbonyl group of Phe^9. Our results, however, did not indicate the presence of such a hydrogen bond, but these amino and carbonyl groups are relatively close to each other in all final six structures.

REFERENCES

[1] Storm, D.R., and Strominger, J.L. (1973) J. Biol. Chem. 248, 3940–3945.
[2] Scogin, D.A., Mosberg, H.I., Strom, D.R., and Gennis, R.B. (1980) Biochemistry 19, 3348–3352.
[3] Redfield, A.G., and Kuntz, S.D. (1975) J. Magn. Reson. 19, 250–254.
[4] Rance, M., Sørensen, O.W., Bodenhausen, G., Wagner, G., Ernst, R.R., and Wüthrich, K. (1983) Biochem. Biophys. Res. Commun. 117, 479–485.
[5] Davis, D.G., and Bax, A. (1985) J. Am. Chem. Soc. 107, 2820–2821.
[6] Macura, S., Huang, Y., Suter, D. and Ernst, R.R. (1981) J. Magn. Reson. 43, 259–281.
[7] Bax, A. and Davis, D.G. (1985) J. Magn. Reson. 63, 207–213.
[8] Brooks, B., Bruccoleri, R.E., Olafson, B.D., States, D.J., Swaminathan, S. and Karplus, M. (1983) J. Comp. Chem. 4, 87–217.
[9] Karplus, M. and McCammon, J.A. (1983) Annu. Rev. Biochem. 53, 263–300.
[10] Mayo, S.L., Olafson, B.D. and Goddard III, W.A. (1990) J. Phys. Chem. 94, 8897–8909.
[11] Wüthrich, K. (1986) NMR of Proteins and Nucleic Acids, Wiley, New York.
[12] Kessler, H., Bats, J.W., Griesinger, C., Koll, S., Klein, M., Will, M. and Wagner, K. (1988) J. Am. Chem. Soc. 110, 1033–1049.
[13] Holak, T.A., Gondol, D., Otlewski, J. and Wilusz, T. (1989) J. Mol. Biol. 210, 635–648.
[14] Clore, G.M., Nilges, M., Sukumaran, D.K., Brünger, A.T., Karplus, M. and Gronenborn, A.M. (1986) EMBO J. 5, 2729–2735.
[15] Zarbock, J., Oschkinat, H., Hannappel, E., Kalbacher, H., Voelter, W. and Holak, T.A. (1989) Biochemistry 29, 7812–7814.
[16] Stanley Jr., R.K., Donna, A.B., Jiri, N., Chinpan, C., Thomas, M.M. and Niels, H.A. (1991) FEBS Lett. 281, 212–218.
[17] Pfeffer, S., Höhne, W., Branner, S., Wilson, K. and Betzel, C. (1991) FEBS Lett. 285, 115–119.
[18] Hausmann, W., Weisiger, J.R. and Craig, L.C. (1955) J. Am. Chem. Soc. 77, 723–731.